# DIFFUSION OF A PASSIVE SCALAR IN A TWO-DIMENSIONAL CHANNEL FLOW

By M. J. MANTON*

[Manuscript received 14 September 1972]

*Abstract*

The asymptotic representation of the distribution of a passive scalar within a two-dimensional channel flow is derived. The distribution is shown to be Gaussian with a skewness and longitudinal variance determined primarily by the mean shear. The distributions corresponding to both laminar and turbulent open channel flows are discussed.

## I. INTRODUCTION

Taylor (1953, 1954) developed a method for predicting the asymptotic state of a passive scalar within a pipe flow and in his treatment considered both the laminar and turbulent cases. A subsequent description of the diffusion process in a duct of variable cross section and arbitrary diffusivity was given by Aris (1956) in terms of the moments of the distribution, but in this case only laminar pipe flow was discussed in detail. The present work considers the diffusion of a passive scalar within a two-dimensional channel flow. The mean distribution of a scalar $\theta$ is assumed to be governed by a diffusion equation with a linear diffusivity, that is, the diffusivity is determined by the flow properties only.

The formal solution of the equation for $\theta$ is obtained in a Fourier integral form. Bounds are determined for the rate of attenuation and the speed of propagation of the Fourier components of $\theta$. Consequently, the asymptotic representation of $\theta$ as time approaches infinity is found to be a Gaussian distribution. The rate of increase in longitudinal variance is determined primarily by the mean shear flow. The mean shear also causes the curve on which $\theta$ is a maximum to be a function of transverse position, i.e. the distribution is skewed. These effects are produced because a finite time is required for the scalar to diffuse transversely from one region of the flow to another.

The distributions of $\theta$ corresponding to laminar and turbulent open channel flows are predicted and the results are compared. The turbulent velocity profile is modelled firstly by the usual logarithmic law and secondly by Prandtl's $\frac{1}{7}$th power law. The turbulent diffusivity is estimated from the Reynolds analogy. The predicted distributions for turbulent flows are compared with the measurements of Elder (1959) and Sullivan (1971).

## II. FORMULATION OF PROBLEM

We consider the diffusion of a passive scalar $\theta$ in the domain $D$ defined by $-\infty < x_1, x_2 < \infty$, $0 < x_3 < H$, and $t > 0$, where $(x_1, x_2, x_3)$ forms a rectangular cartesian coordinate system and $t$ is time. The mean distribution of $\theta$ within the

* Department of Mathematics, Monash University, Clayton, Vic. 3168.

domain $D$ is governed by the equation

$$\frac{\partial\theta}{\partial t}+u\frac{\partial\theta}{\partial x_1}=\frac{\partial}{\partial x_1}\left(K_1^*\frac{\partial\theta}{\partial x_1}\right)+\frac{\partial}{\partial x_2}\left(K_2^*\frac{\partial\theta}{\partial x_2}\right)+\frac{\partial}{\partial x_3}\left(K_3^*\frac{\partial\theta}{\partial x_3}\right), \tag{1}$$

where $\boldsymbol{u} = (u(x_3), 0, 0)$ is the mean velocity vector of the fluid and $K_i^*(x_3)$ $(i = 1, 2, 3)$ is the diffusivity of $\theta$ in the $x_i$ direction.

For the scalar to be conserved, there must be no flux of $\theta$ through the boundaries of the flow and hence

$$\partial\theta/\partial x_3 = 0 \qquad \text{on} \qquad x_3 = 0, H. \tag{2}$$

The initial distribution of $\theta$ is such that

$$\theta = \Theta_0(\boldsymbol{x}) \qquad \text{at} \qquad t = 0. \tag{3}$$

The initial distribution is assumed to be centred on the $x_3$ axis and the total amount of the scalar is assumed to be finite. We now seek a bounded solution of the parabolic system defined by equations (1)–(3).

To facilitate discussion, we introduce the normalized variables

$$\left.\begin{aligned}(x,y,z) = (x_1/H, x_2/H, x_3/H), \qquad & \theta_0(x,y,z) = \Theta_0(\boldsymbol{x}),\\ \tau = \nu t/H^2, \qquad v(z) = uH/\nu, \qquad & K_i(z) = K_i^*/\nu,\end{aligned}\right\} \tag{4}$$

where $\nu$ is the molecular viscosity of the fluid and $\theta$ is normalized such that

$$\int_0^1 \mathrm{d}z \iint_{-\infty}^{\infty} \mathrm{d}x\,\mathrm{d}y\,\theta(x,y,z) = 1.$$

From the definitions (4), the system (1)–(3) in $D$ becomes

$$\frac{\partial\theta}{\partial\tau}+v\frac{\partial\theta}{\partial x}=K_1\frac{\partial^2\theta}{\partial x^2}+K_2\frac{\partial^2\theta}{\partial y^2}+\frac{\partial}{\partial z}\left(K_3\frac{\partial\theta}{\partial z}\right) \tag{5}$$

with

$$\partial\theta/\partial z = 0 \qquad \text{on} \qquad z = 0, 1;$$

$$\theta = \theta_0(x,y,z) \qquad \text{at} \qquad \tau = 0.$$

Because $\theta$ is bounded, equation (5) may be transformed to yield

$$\frac{\partial}{\partial z}\left(K_3\frac{\partial\tilde\theta}{\partial z}\right)-(K_1k^2+K_2l^2+s-\mathrm{i}kv)\tilde\theta(z;s,k,l) = -\tilde\theta_0(z;k,l) \tag{6}$$

with

$$\partial\theta/\partial z = 0 \qquad \text{on} \qquad z = 0, 1,$$

where

$$\tilde\theta(z;s,k,l) = \int_0^\infty \mathrm{d}\tau\,\exp(-s\tau)\iint_{-\infty}^{\infty}\mathrm{d}x\,\mathrm{d}y\,\exp(\mathrm{i}kx+\mathrm{i}ly)\,\theta(x,y,z,\tau)$$

and

$$\tilde\theta_0(z;k,l) = \iint_{-\infty}^{\infty}\mathrm{d}x\,\mathrm{d}y\,\exp(\mathrm{i}kx+\mathrm{i}ly)\,\theta_0(x,y,z).$$

We now restrict discussion to the homogeneous system corresponding to (6), namely

$$(K_3 f')' - (K_1 k^2 + K_2 l^2 + s - ikv) f(z) = 0, \tag{7}$$

with $f' = 0$ on $z = 0, 1$. In this equation $s$ is an eigenvalue and $f$ is its associated eigenfunction, while the prime denotes differentiation with respect to $z$. Such a restriction is valid because the eigenfunctions of (7) are orthogonal and so $\tilde{\theta}$ in (6) may be represented by its eigenfunction expansion.

The orthogonality of two distinct eigenfunctions $f_n$ and $f_m$ is seen by setting $f = f_n$ in equation (7). Then

$$f_m\{(K_3 f_n')' - (K_1 k^2 + K_2 l^2 + s_n - ikv) f_n\} = 0,$$

and similarly

$$f_n\{(K_3 f_m')' - (K_1 k^2 + K_2 l^2 + s_m - ikv) f_m\} = 0.$$

Subtracting these equations and using the boundary conditions on $f$, we find that

$$(s_n - s_m) \int_0^1 \mathrm{d}z\, f_n f_m = 0,$$

that is, $f_n$ and $f_m$ are orthogonal provided that the eigenvalues $s_n$ and $s_m$ are distinct.

If $\{f_n, n = 0, 1, 2, \ldots\}$ is the set of eigenfunctions of (7) then $\tilde{\theta}_0$ has the expansion

$$\tilde{\theta}_0 = \sum_{n=0}^{\infty} b_n(k, l) f_n(z; k, l), \tag{8}$$

where

$$b_n = \int_0^1 \mathrm{d}z\, \tilde{\theta}_0(z) f_n(z) \Big/ \int_0^1 \mathrm{d}z\, f_n^2(z).$$

From equations (6)–(8) it is seen that

$$\tilde{\theta}(z; s, k, l) = \sum_{n=0}^{\infty} b_n(k, l) f_n(z; k, l)/(s - s_n).$$

Applying an inverse transform to this expression, we find that

$$\theta(x, y, z, \tau) = \sum_{n=0}^{\infty} (2\pi)^{-2} \iint_{-\infty}^{\infty} \mathrm{d}k\, \mathrm{d}l \exp\{-ikx - ily + \tau s_n(k, l)\}\, b_n(k, l) f_n(z; k, l). \tag{9}$$

Equation (9) is the formal solution for $\theta$ in terms of its initial distribution.

Limits are found now for the real and imaginary parts of the eigenvalue $s$. Multiplying equation (7) by $f^*$, the complex conjugate of $f$, integrating with respect to $z$, and applying the boundary conditions, we see that

$$\int_0^1 \mathrm{d}z\, \{K_3 |f'|^2 + (K_1 k^2 + K_2 l^2 + s - ikv)|f|^2\} = 0. \tag{10}$$

Clearly, the real and imaginary parts of this expression must be zero independently.

Hence

$$\int_0^1 \mathrm{d}z\,\{K_3|f'|^2+(K_1k^2+K_2l^2+s_r)|f|^2\} = 0 \tag{11a}$$

and

$$\int_0^1 \mathrm{d}z\,(s_i-kv)|f|^2 = 0, \tag{11b}$$

where $s = s_r+is_i$ with $s_r$ and $s_i$ real. If we have $0 < K_{i,\min} < K_i(z)$ and $v_{\min} < v(z) < v_{\max}$ for $0 < z < 1$ then equations (11) imply that

$$s_r < -(K_{1,\min}k^2+K_{2,\min}l^2) \qquad \text{and} \qquad v_{\min} < s_i/k < v_{\max}. \tag{12a, b}$$

Inequality (12a) gives a lower bound on the attenuation rate of the Fourier components of $\theta$ while (12b) implies that the phase speed of a component is equal to the fluid speed at some point in the flow.

For the trivial case in which $v$, $K_1$, and $K_2$ are all independent of $z$, equation (10) yields $s_r \leqslant -(K_1k^2+K_2l^2)$ and $s_i/k = v$. The equality is included in the first expression because an eigenfunction is $f' \equiv 0$, that is, $f(z) = 1$.

## III. Asymptotic Distribution

It can be seen from equations (9) and (12) that as $\tau$ approaches infinity the main contribution to $\theta$ will be from the low wave-number components of each eigenfunction, that is, the small scale components of the initial distribution, corresponding to large values of $k$ and $l$, are rapidly attenuated by diffusion. Therefore, it would seem to be useful to consider the solutions of equation (7) for small values of $k$ and $l$.

When $k$ and $l$ are identically zero, the first (least oscillatory) eigenfunction of equation (7) is

$$(f_0)_{k=0=l} = 1 \tag{13}$$

with the associated eigenvalue $(s_0)_{k=0=l} = 0$. For all other eigenfunctions equation (11a) shows that $s_r$ is negative. However, equation (9) implies that the dominant eigenfunction as $\tau \to \infty$ is that function whose eigenvalue has the largest real part. Clearly, the first eigenfunction (13) is dominant. Thus, we consider an asymptotic expansion of the dominant eigenfunction of equation (7) as $k$ and $l$ approach zero.

We seek a solution of the form

$$f_0(z;k,l) = \exp g(z;k,l), \tag{14}$$

where $g(z;0,0) = 0$ and so $f(z;0,0) = 1$. Substituting equation (14) into (7), we find the expression for the function $g(z)$

$$(K_3g')'+K_3g'^2 = K_1k^2+K_2l^2+s_0-ikv \tag{15}$$

with

$$g' = 0 \qquad \text{on} \qquad z = 0,1.$$

We write

$$l = \alpha k \qquad \text{with} \qquad \alpha = O(1), \tag{16}$$

and the function $g$ and the eigenvalue $s_0$ are expanded in asymptotic power series in $k$ as

$$g(z;k,l) = \sum_{n=1}^{\infty} k^n g_n(z;\alpha), \qquad s_0(k,l) = \sum_{n=1}^{\infty} k^n s_n(\alpha). \tag{17}$$

By substituting (16) and (17) into (15) and equating the coefficients of like powers of $k$, a sequence of equations for the set $\{(g_n, s_n), n = 1,2,...\}$ is determined. The first two of these equations are

$$(K_3 g_1')' = s_1 - \mathrm{i}v, \tag{18a}$$

$$(K_3 g_2')' = s_2 + K_1 + \alpha^2 K_2 - K_3 g_1'^2. \tag{18b}$$

The boundary conditions on $g$ become

$$g_n' = 0 \qquad \text{on} \qquad z = 0,1, \qquad n = 1,2,.... \tag{19}$$

Integrating equation (18a) and using the conditions (19), we find that

$$K_3 g_1' = s_1 z - \mathrm{i}\int_0^z v(\zeta)\,\mathrm{d}\zeta,$$

where

$$s_1 = \mathrm{i}\int_0^1 v(z)\,\mathrm{d}z. \tag{20}$$

Thus equation (20) implies that, to order $k$ at least, the phase speed of a large scale component of $\theta$ is equal to the mean fluid speed within the channel. This clearly satisfies the condition (12b). Another integration yields

$$g_1(z) = \mathrm{i}\int_0^z \frac{\zeta}{K_3(\zeta)}\left(\int_0^1 v(\zeta_1)\,\mathrm{d}\zeta_1 - \zeta^{-1}\int_0^\zeta v(\zeta_1)\,\mathrm{d}\zeta_1\right)\mathrm{d}\zeta, \tag{21}$$

where the constant of integration has been set equal to zero without loss of generality.

Similarly, the system (18b) and (19) may be solved to give

$$\begin{aligned} s_2(\alpha) = &-\int_0^1 \{K_1(z) + \alpha^2 K_2(z)\}\,\mathrm{d}z \\ &-\int_0^1 \frac{z^2}{K_3(z)}\left(\int_0^1 v(\zeta)\,\mathrm{d}\zeta - z^{-1}\int_0^z v(\zeta)\,\mathrm{d}\zeta\right)^2 \mathrm{d}z \end{aligned} \tag{22}$$

and

$$\begin{aligned} g_2(z;\alpha) = &-\int_0^z \frac{\zeta}{K_3(\zeta)}\left(\int_0^1 \{K_1(\zeta_1) + \alpha^2 K_2(\zeta_1)\}\,\mathrm{d}\zeta_1\right. \\ &\left. \qquad -\zeta^{-1}\int_0^\zeta \{K_1(\zeta_1) + \alpha^2 K_2(\zeta_1)\}\,\mathrm{d}\zeta_1\right)\mathrm{d}\zeta \\ &-\int_0^z \frac{\zeta}{K_3(\zeta)}\left\{\int_0^1 \frac{\zeta_1^2}{K_3(\zeta_1)}\left(\int_0^1 v(\zeta_2)\,\mathrm{d}\zeta_2 - \zeta_1^{-1}\int_0^{\zeta_1} v(\zeta_2)\,\mathrm{d}\zeta_2\right)^2 \mathrm{d}\zeta_1\right. \\ &\left. \qquad -\zeta^{-1}\int_0^\zeta \frac{\zeta_1^2}{K_3(\zeta_1)}\left(\int_0^1 v(\zeta_2)\,\mathrm{d}\zeta_2 - \zeta^{-1}\int_0^{\zeta_1} v(\zeta_2)\,\mathrm{d}\zeta_2\right)^2 \mathrm{d}\zeta_1\right\}\mathrm{d}\zeta. \end{aligned} \tag{23}$$

Therefore $s_2$ is negative and satisfies the condition (12a). The dominant eigenfunction $f_0$ and its associated eigenvalue $s_0$ are given to order $k^2$ by equations (14), (16), (17), and (20)–(23).

It has been seen above that as $\tau \to \infty$ the formal solution (9) is dominated by the first term of the eigenfunction expansion, i.e. as $\tau \to \infty$

$$\theta \sim (2\pi)^{-2} \iint_{-\infty}^{\infty} \mathrm{d}k\,\mathrm{d}l \exp(-\mathrm{i}kx - \mathrm{i}ly + s_0\tau)\, b_0(k,l) f_0(z;k,l). \tag{24}$$

Equations (6), (8), (14), and (17) imply that

$$\begin{aligned} b_0 &= \int_0^1 \mathrm{d}z\, \tilde{\theta}_0(z;0,0) + O(k) + O(l) \\ &= \int_0^1 \mathrm{d}z \iint_{-\infty}^{\infty} \mathrm{d}x\,\mathrm{d}y\, \theta_0(x,y,z) + O(k) + O(l) \\ &= 1 + O(k) + O(l). \end{aligned} \tag{25}$$

Therefore, the asymptotic distribution of the scalar is found from equations (17), (24), and (25) to be

$$\begin{aligned} \theta \sim (2\pi)^{-2} \iint_{-\infty}^{\infty} \mathrm{d}k\,\mathrm{d}l \exp[&-\mathrm{i}kx - \mathrm{i}ly + \tau\{ks_1 + k^2 s_2(l/k) + O(k^3)\} \\ &+ kg_1(z) + k^2 g_2(z;l/k) + O(k^3)] \\ \times \{1 &+ O(k) + O(l)\}. \end{aligned} \tag{26}$$

For large $\tau$ the integrand in (26) is attenuated rapidly away from the point $k = 0 = l$ and we may thus use Laplace's method (see e.g. Carrier *et al.* 1966) to approximate the integral. Equation (26) then becomes

$$\theta \sim (4\pi XY)^{-1} \exp(-M^2/4X^2 - y^2/4Y^2), \tag{27}$$

where

$$\begin{aligned} X^2(z,\tau) &= \tau(\bar{K}_1 + \bar{K}_{\mathrm{app}}) + \int_0^z \{\zeta/K_3(\zeta)\}\langle K_1(\zeta)\rangle\, \mathrm{d}\zeta \\ &\quad + \int_0^z \{\zeta/K_3(\zeta)\}\langle K_{\mathrm{app}}(\zeta)\rangle\, \mathrm{d}\zeta, \\ Y^2(z,\tau) &= \tau\bar{K}_2 + \int_0^z \{\zeta/K_3(\zeta)\}\langle K_2(\zeta)\rangle\, \mathrm{d}\zeta, \\ M(x,z,\tau) &= \tau\bar{v} - x + \int_0^z \{\zeta/K_3(\zeta)\}\langle v(\zeta)\rangle\, \mathrm{d}\zeta. \end{aligned}$$

Here $\bar{m}$ denotes the overall average value of the function $m$,

$$\bar{m} = \int_0^1 m(z)\, \mathrm{d}z, \tag{28}$$

while $\langle m(z)\rangle$ denotes a local average of $m$ relative to the overall average value $\bar{m}$,

$$\langle m(z)\rangle = \int_0^1 m(\zeta)\,\mathrm{d}\zeta - z^{-1}\int_0^z m(\zeta)\,\mathrm{d}\zeta, \tag{29}$$

that is, $\langle m\rangle$ is the difference between the average values of $m$ over the intervals $(0,1)$ and $(0,z)$. The mean shear flow produces an apparent diffusivity $K_{\mathrm{app}}$ given by

$$K_{\mathrm{app}}(z) = \{z^2/K_3(z)\}\langle v(z)\rangle^2. \tag{30}$$

Clearly, the asymptotic distribution of $\theta$ is Gaussian, centred on the curve $y = 0 = M(x,z,\tau)$, with variances $Y^2$ in the $y$ direction and $X^2$ in the $x$ direction. The speed of propagation of the distribution is equal to $\bar{v}$, the average fluid speed in the flow. Because of the mean shear, the position of the maximum value of $\theta$ depends upon $z$. This position varies as the product of the diffusion time scale $z^2/K_3$ and the horizontal velocity scale $\langle v(z)\rangle$, that is, although the flow may be well mixed the maximum in $\theta$ varies with $z$ because a finite time is required for a parcel of scalar to move in the $z$ direction by diffusion from one position to another.

The variance $Y^2$ in the $y$ direction is essentially equal to $\tau\bar{K}_2$, the product of the time and the average diffusivity. If $K_2$ is a function of $z$ then $Y^2$ also varies in the $z$ direction. The variation has the magnitude of the diffusion time $z^2/K_3$ multiplied by the change in $K_2$ over the interval $(0,z)$, i.e. it is of order $(z^2/K_3)\langle K_2\rangle$.

The leading term in the variance $X^2$ is equal to $\tau(\bar{K}_1+\bar{K}_{\mathrm{app}})$. Thus, in addition to the term proportional to the average diffusivity in the $x$ direction, the variance is increased by a term proportional to the average value of the apparent diffusivity. The apparent diffusivity is caused by the mean shear and it is equal to the product of the diffusion time scale $z^2/K_3$ and the average square velocity scale $\langle v\rangle^2$ over the interval $(0,z)$. The variance $X^2$ depends weakly upon $z$ provided that $K_1$ and $K_{\mathrm{app}}$ depend upon $z$.

## IV. Examples

To investigate the dependence of the asymptotic distribution of a scalar upon the flow conditions in a two-dimensional open channel, we consider some simple examples. In particular, the rate of increase in longitudinal variance

$$\mathrm{d}(X^2)/\mathrm{d}\tau = \bar{K}_1+\bar{K}_{\mathrm{app}} \tag{31}$$

and the curve of maximum $\theta$

$$M(x,z,\tau) = 0 \tag{32}$$

are calculated.

(i) A laminar flow driven by a constant pressure gradient is described by

$$v = 3R(z-\tfrac{1}{2}z^2) \qquad \text{and} \qquad K_1 = K_2 = K_3 = Sc^{-1}, \tag{33}$$

where $R$ is the Reynolds number of the flow based on the average fluid speed in the channel ($R = \bar{v}$) and $Sc$ is the constant Schmidt number of the scalar $\theta$ within the fluid. Substituting the relations (33) into equation (27) with the associated definitions and equations (31) and (32), we find that

$$\mathrm{d}(X^2)/\mathrm{d}\tau = Sc^{-1} + \tfrac{2}{105} R^2\, Sc \tag{34}$$

and that the curve of maximum $\theta$ is

$$x - R\tau = \tfrac{1}{2} R\, Sc\,(z^2 - z^3 + \tfrac{1}{4} z^4). \tag{35}$$

Thus, the maximum in $\theta$ at the free surface ($z = 1$) occurs at $\frac{1}{8} R\, Sc$ channel depths downstream of that at the bottom of the flow ($z = 0$), i.e. the distribution of $\theta$ is skewed with a tail of length $\frac{1}{8} R\, Sc$ channel depths.

(ii) For a laminar flow driven by a constant stress at the surface, we have

$$v = 2Rz \qquad \text{and} \qquad K_1 = K_2 = K_3 = Sc^{-1}. \tag{36}$$

In this case, it is found that

$$\mathrm{d}(X^2)/\mathrm{d}\tau = Sc^{-1} + \tfrac{1}{30} R^2\, Sc \tag{37}$$

and the curve of maximum $\theta$ is

$$x - R\tau = R\, Sc\,(\tfrac{1}{2} z^2 - \tfrac{1}{3} z^3). \tag{38}$$

This distribution has a tail of length $\frac{1}{6} R\, Sc$ channel depths. From equations (34) and (35) and (37) and (38) it is seen that a linear velocity profile produces more diffusion of a scalar than does a parabolic profile at the same Reynolds and Schmidt numbers.

A fully developed turbulent flow in an open channel is characterized by the kinematic shear stress $(u^*)^2$ at the bottom of the channel. The mean fluid velocity is found to be represented well by the familiar logarithmic profile for boundary layers (Elder 1959; Sullivan 1971), namely

$$v = \{\kappa^{-1} \ln(v^* z) + a\} v^*, \tag{39}$$

where $v^* = u^* H/\nu$ and $\kappa$ and $a$ are constants. The normalized friction velocity $v^*$ is related to the Reynolds number $R$ by the relation

$$R = v^* \{\kappa^{-1}(\ln v^* - 1) + a\}. \tag{40}$$

This expression allows $\mathrm{d}(X^2)/\mathrm{d}\tau$ to be expressed in terms of $R$ rather than $v^*$.

To estimate the vertical turbulent diffusivity, we apply the Reynolds analogy such that

$$K_3 = T(\mathrm{d}v/\mathrm{d}z)^{-1}, \tag{41}$$

where $T(z)$ is the normalized kinematic shear stress. Because the molecular diffusivity is generally several orders of magnitude smaller than the turbulent diffusivity, the effect of the former is neglected.

To evaluate $\mathrm{d}(X^2)/\mathrm{d}\tau$, the longitudinal turbulent diffusivity $K_1$ must be specified also. The contribution of $K_1$ to $\mathrm{d}(X^2)/\mathrm{d}\tau$ is usually small compared with that from

$K_{app}$ and so a simple model for $K_1$ may be used. Thus, the turbulent diffusivity of $\theta$ is assumed to be isotropic such that

$$K_1 = K_3. \tag{42}$$

(iii) In an open channel flow driven by a constant pressure gradient, the stress is given by

$$T = (v^*)^2(1-z). \tag{43}$$

It then follows from equations (39), (41), and (43) that the diffusivity in a flow with a logarithmic velocity and a linear stress is

$$K_3 = \kappa v^* z(1-z). \tag{44}$$

Substituting equations (39) and (44) into (30), we find that

$$\bar{K}_{app} = \tfrac{1}{4}v^*\kappa^{-3} \sum_{n=0}^{\infty} 8(n+2)^{-3}. \tag{45}$$

Equation (45) for the average apparent diffusivity has been given by Elder (1959), who applied a method developed by Taylor (1954). The rate of increase in longitudinal variance is calculated from equations (31), (42), (44), and (45) to be

$$\mathrm{d}(X^2)/\mathrm{d}\tau = \left(\tfrac{1}{6}\kappa + \tfrac{1}{4}\kappa^{-3} \sum_{n=0}^{\infty} 8(n+2)^{-3}\right)v^*. \tag{46}$$

(iv) For a turbulent flow driven by a constant stress,

$$T = (v^*)^2 \tag{47}$$

and hence, for a logarithmic velocity,

$$K_3 = \kappa v^* z. \tag{48}$$

From equations (30), (39), and (48) the average apparent diffusivity for a constant stress flow is

$$\bar{K}_{app} = \tfrac{1}{4}v^*\kappa^{-3},$$

which is somewhat less than $\bar{K}_{app}$ for a linear stress flow. Using assumption (42), we finally obtain

$$\mathrm{d}(X^2)/\mathrm{d}\tau = (\tfrac{1}{2}\kappa + \tfrac{1}{4}\kappa^{-3})v^*. \tag{49}$$

Because the logarithmic velocity is unbounded as $z \to 0$, curves of maximum $\theta$ cannot be estimated without the use of an additional assumption about the behaviour of the mean velocity in the viscous sublayer. However, the mean velocity profile in the wall region of a boundary layer is found to represented well by Prandtl's $\frac{1}{7}$th power law (Hinze 1959), namely

$$v = \tfrac{8}{7}Rz^{1/7}, \tag{50}$$

where $R = \frac{7}{8}C(v^*)^{8/7}$ and $C$ is a constant. Equation (50) fits the experimental boundary layer data as well as the logarithmic law (39) and, being algebraic and not infinite at $z = 0$, it is more amenable.

(v) For the linear stress (43) it is found from equations (41) and (50) that

$$K_3 = \frac{7}{C}\left(\frac{8R}{7C}\right)^{3/4}(1-z)z^{6/7}.$$

Hence

$$\frac{\mathrm{d}(X^2)}{\mathrm{d}\tau} = \frac{343}{260\,C}\left(\frac{8}{7C}\right)^{3/4}R^{3/4} + \frac{C}{2040}\left(\frac{7C}{8}\right)^{3/4}R^{5/4}\sum_{n=0}^{\infty}\frac{4080}{(7n+15)(7n+16)(7n+17)} \tag{51}$$

and a curve of maximum $\theta$ is

$$x-R\tau = C\left(\frac{7C}{8}\right)^{3/4}R^{1/4}\sum_{n=0}^{\infty}\left(\frac{z^{(7n+8)/7}}{7n+8}-\frac{z^{(7n+9)/7}}{7n+9}\right). \tag{52}$$

(vi) A constant stress flow (47) produces a turbulent diffusivity

$$K_3 = \frac{7}{C}\left(\frac{8R}{7C}\right)^{3/4}z^{6/7}$$

and therefore

$$\frac{\mathrm{d}(X^2)}{\mathrm{d}\tau} = \frac{49}{13\,C}\left(\frac{8}{7C}\right)^{3/4}R^{3/4}+\frac{C}{2040}\left(\frac{7C}{8}\right)^{3/4}R^{5/4}. \tag{53}$$

The corresponding curve of maximum $\theta$ is

$$x-R\tau = C\left(\frac{7C}{8}\right)^{3/4}R^{1/4}\left(\tfrac{1}{8}z^{8/7}-\tfrac{1}{9}z^{9/7}\right). \tag{54}$$

## V. Discussion

At the same Reynolds and Schmidt numbers, equations (33)–(38) show that a laminar flow with a linear velocity profile (constant stress) produces more diffusion of a scalar than one with a parabolic profile (linear stress). However, if the Reynolds number $R$ based on the average velocity is replaced by that based on the maximum velocity $v_{\max}$ then in both cases the rate of increase in variance is given by

$$\mathrm{d}(X^2)/\mathrm{d}\tau \approx Sc^{-1}+\tfrac{1}{120}v_{\max}^2\,Sc.$$

Similarly, the distribution has a tail of length $\frac{1}{12}v_{\max}Sc$ channel depths. Thus, the maximum fluid velocity rather than the average velocity would seem to be the characteristic velocity required to describe the diffusion of a scalar in a laminar open channel flow.

The variation of $\mathrm{d}(X^2)/\mathrm{d}\tau$ with Reynolds number $R$ is shown in Figure 1 for the examples considered in Section IV. The Schmidt number $Sc$ is taken equal to unity for comparison of the laminar and turbulent cases. The constants appearing in the equations for the turbulent flows have their usual experimental values: $\kappa^{-1} = 2\cdot43$ and $a = 4\cdot9$ (Sullivan 1971) and $C = 8\cdot3$ (Hinze 1959).

It is clear from Figure 1 that if a flow can exist in either the laminar or turbulent regime at the same Reynolds number then the former regime produces the greater diffusion of a scalar. This occurs because, firstly, the vertical diffusion time is much greater for a laminar flow ($[K_3]_{lam} \ll [K_3]_{turb}$) and, secondly, the average velocity difference across the flow is larger for a laminar flow than for the corresponding turbulent flow; in particular, $v_{max}$ is equal to $\frac{8}{7}R$ for the turbulent velocity (50) whereas it has values of $2R$ and $\frac{3}{2}R$ for linear and parabolic velocity profiles respectively.

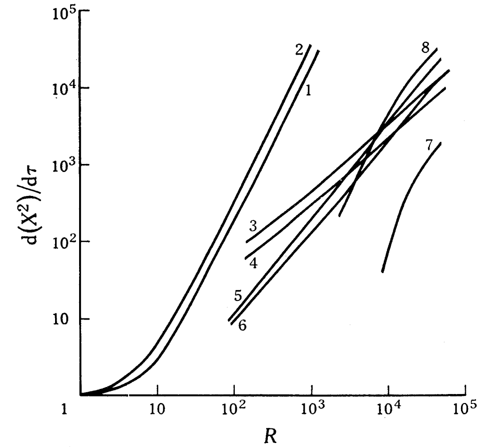


Fig. 1.—Dependence of rate of increase in longitudinal variance $X^2$ with Reynolds number $R$:

1, laminar parabolic velocity;
2, laminar linear velocity;
3, logarithmic velocity, linear shear stress;
4, logarithmic velocity, constant shear stress;
5, $\frac{1}{7}$th power law velocity, linear shear stress;
6, $\frac{1}{7}$th power law velocity, constant shear stress;
7, Sullivan (1971), first stage;
8, Sullivan (1971), second stage.

In the laminar case, a constant stress flow produces more diffusion than a linear stress flow ($d(X^2)/d\tau$ is increased by a factor of $1\cdot75$ for large Reynolds number), whereas the converse is true in the turbulent case. This arises because the diffusivity $K_3$ is fixed but the velocity $v$ varies with the stress for laminar flows while, on the other hand, $K_3$ varies with the stress but $v$ is fixed in the turbulent case. When the turbulent velocity is represented by a logarithmic profile, $d(X^2)/d\tau$ is $1\cdot54$ times larger for a linear stress flow than for the corresponding constant stress flow. This factor approaches $1\cdot74$ as $R \to \infty$ for a $\frac{1}{7}$th power law velocity. Thus, the particular representation of the diffusivity $K_3$ does not greatly affect the rate of increase in longitudinal variance $d(X^2)/d\tau$.

The results associated with the different representations of the turbulent velocity profile should be compared only over the Reynolds number range for which the profiles coincide. The following tabulation shows the variation of $R$ with the friction velocity $v^*$.

| $v^*$ | 20 | 50 | 100 | 200 | 500 | 1000 | 2000 |
|---|---|---|---|---|---|---|---|
| $R$ (log law) | 195 | 600 | 1370 | 3070 | 8790 | 19260 | 41900 |
| $R$ ($\frac{1}{7}$th law) | 223 | 635 | 1400 | 3090 | 8820 | 19470 | 43000 |

We see that at $v^* = 20$ the Reynolds number derived from the logarithmic law (40) is over 10% less than that from the $\frac{1}{7}$th law (50). The corresponding value of $d(X^2)/d\tau$ is at least four times greater than that derived from (50). This discrepancy decreases with increasing $v^*$ such that at a friction velocity $v^*$ of about 500 the difference in

Reynolds number is less than $0 \cdot 5\%$ and the difference in $\mathrm{d}(X^2)/\mathrm{d}\tau$ is less than $10\%$. Thus $\mathrm{d}(X^2)/\mathrm{d}\tau$ appears to be quite sensitive to the precise form of the velocity profile.

The actual behaviour of $\mathrm{d}(X^2)/\mathrm{d}\tau$ does not seem as yet to be determined exactly from experiments. Elder (1959) found equation (46) (i.e. curve 3 in Fig. 1) to give a good representation of $\mathrm{d}(X^2)/\mathrm{d}\tau$. However, Sullivan (1971) found that the behaviour of $\mathrm{d}(X^2)/\mathrm{d}\tau$ varies with the diffusion time. Curve 7 in Figure 1 is the result for Sullivan's first stage of development, which is defined by $0 \cdot 5 < v^*\tau < 4$. These values of $\mathrm{d}(X^2)/\mathrm{d}\tau$ are at least 10 times smaller than the predicted values. On the other hand, the diffusion process has not reached an asymptotic state at this stage and so the analysis of Section III is not expected to apply without the addition of further terms in the asymptotic expansion for $\theta$.

The behaviour of $\mathrm{d}(X^2)/\mathrm{d}\tau$ in Sullivan's (1971) second stage is shown by curve 8 in Figure 1. In this case the value of $\mathrm{d}(X^2)/\mathrm{d}\tau$ is of the same order of magnitude as the predicted values. For large Reynolds numbers, Sullivan's result is somewhat like curve 5, i.e. the $\frac{1}{7}$th power law result (51).

From the curve of maximum $\theta$, given by equation (52), the tail of the distribution in a turbulent flow with a linear stress is found to be of length $0 \cdot 9\, R^{1/4}$ channel depths. The corresponding result for a constant stress flow is $0 \cdot 5\, R^{1/4}$ channel depths. We note that the tail length in a laminar flow is proportional to $R$, that is, a laminar flow produces more diffusion than a turbulent flow at the same Reynolds number. The skewness in the distribution of $\theta$ caused by the tail must persist because a finite time is required for a scalar to diffuse vertically from one region to another. However, as $\tau$ increases, the standard deviation of the distribution of $\theta$ becomes much larger than the length of the tail and this could make the tail difficult to distinguish experimentally.

Measured distributions of $\theta$ for $v^*\tau \lesssim 30$ are found to have tails. Elder (1959) proposed that the skewness is caused by a scalar trapped in the viscous sublayer. To show that the sublayer plays a minor role in the distribution of the scalar in a turbulent channel, we consider a $\frac{1}{7}$th law profile matched to a linear viscous profile:

$$\begin{aligned} v &= (v^*)^2 z, & 0 < z < z_0, \\ &= C(v^*)^{8/7} z^{1/7}, & z_0 < z < 1, \end{aligned}$$

where $z_0 = C^{7/6}/v^*$. The ratio of the mass flux in the sublayer to that in the turbulent region for this profile is

$$\begin{aligned} \gamma &= \int_0^{z_0} v(z)\, \mathrm{d}z \Big/ \int_{z_0}^{1} v(z)\, \mathrm{d}z \\ &= \tfrac{4}{7} C^{4/3} \{(v^*)^{8/7} - C^{4/3}\}^{-1}. \end{aligned}$$

Taking $C = 8 \cdot 3$ gives $\gamma \sim 3 \cdot 5 \times 10^{-3}$ for a friction velocity $v^* \sim 10^3$, that is, a negligible fraction of the fluid (and hence of the scalar) resides in the sublayer at high Reynolds numbers. The unimportance of the sublayer to the diffusion process has been pointed out also by Sullivan (1971).

The length of the distribution tail calculated for a $\frac{1}{7}$th power law velocity is an underestimate of the actual length of the tail in a turbulent channel flow. This is because the $\frac{1}{7}$th law overestimates the mean fluid velocity near the wall, in particular, for $v^*z \lesssim 50$ (Hinze 1959). On the other hand, the tails of experimentally measured distributions are found to have lengths much greater than the predicted value of $0 \cdot 9\, R^{1/4}$. For example, at a Reynolds number of $10^4$ the predicted tail length is 9 channel depths whereas Sullivan (1971) has measured a corresponding length of 20–30 channel depths. However, Sullivan's measurements were taken during his first stage of development, i.e. before the distribution acquired its asymptotic state.

It is seen from equation (5) that the relative magnitude of the advection term to the diffusion terms in the relation for $\theta$ is equal to $v/K_3$, which is of order $R/v^*$ for a turbulent flow. Because this ratio is large there is an initial period after the release of the scalar into the flow during which the diffusion terms in the equation for $\theta$ are relatively unimportant, that is, the distribution of scalar for small times is approximated by

$$\theta \approx \theta_0(x - v\tau, y, z),$$

where $\theta_0(x, y, z)$ is the initial distribution of $\theta$. This approximation is valid for $0 < K_3\tau \lesssim 1$, i.e. for $0 < v^*\tau \lesssim 1$.

If the scalar initially spans the channel then the distribution produces a tail of length $\tau v_{\max}$ during the initial period. The distribution of $\theta$ therefore develops a tail of order $v_{\max}/v^*$ in length before the diffusion processes begin to dominate. Thus the tail observed by Elder (1959) and Sullivan (1971) is probably the remnant of this initial tail. The initial tail is not smoothed out until the standard deviation of the distribution becomes comparable with the tail length, that is, the asymptotic state is reached only when

$$X^2 \sim v_{\max}/v^*.$$

From equations (27), (50), and (51) with $C = 8 \cdot 3$, this condition becomes

$$v^*\tau \sim 200\,(v^*)^{-1/7}. \tag{55}$$

Thus for $v^* \sim 10^3$ equation (55) predicts that the final asymptotic state of development of the distribution will occur for $v^*\tau \sim 75$, which is somewhat later than the value of $v^*\tau \sim 30$ given by Sullivan (1971).

We note finally that the quantity measured by Elder (1959) and Sullivan (1971) is the average distribution $\bar{\theta}$ given by

$$\bar{\theta} = \int_0^1 \theta \,\mathrm{d}z.$$

It is clear from equation (27) that $\bar{\theta}$ does not have a simple Gaussian behaviour. Because of the tail in the $\theta$ distribution, $\bar{\theta}$ is also skewed. In addition, the time dependence of the peak value of $\bar{\theta}$ does not vary simply as $(XY)^{-1}$, that is, as $t^{-1}$. Sullivan has reported that the peak value decreases more quickly than that for a Gaussian distribution.

## VI. References


Aris, R. (1956).—*Proc. R. Soc.* A **235**, 67.

Carrier, G. F., Krook, M., and Pearson, C. E. (1966).—"Functions of a Complex Variable." (McGraw–Hill: New York.)

Elder, J. W. (1959).—*J. Fluid Mech.* **5**, 544.

Hinze, J. O. (1959).—"Turbulence." (McGraw–Hill: New York.)

Sullivan, P. J. (1971).—*J. Fluid Mech.* **49**, 551.

Taylor, G. I. (1953).—*Proc. R. Soc.* A **219**, 186.

Taylor, G. I. (1954).—*Proc. R. Soc.* A **223**, 446.